Cerebral Cortex, April 2018;28: 1132–1140

doi: 10.1093/cercor/bhx021
Advance Access Publication Date: 10 February 2017
Original Article

ORIGINAL ARTICLE

Cognitive Enhancement Induced by Anodal tDCS Drives Circuit-Specific Cortical Plasticity

Alberto Pisoni[1,2], Giulia Mattavelli[1,2], Costanza Papagno[1,2,6], Mario Rosanova[3,4], Adenauer G. Casali[5] and Leonor J. Romero Lauro[1,2]

[1]Department of Psychology, Università degli Studi di Milano-Bicocca, Milano 20126, Italy, [2]NeuroMi, Milan Center for Neuroscience, Milano 20126, Italy, [3]Department of Clinical Sciences, "Luigi Sacco", Università degli Studi di Milano, Milano 20157, Italy, [4]Fondazione Europea di Ricerca Biomedica, FERB Onlus, Cernusco sul Naviglio 20063, Milano, Milano, Italy, [5]Institute of Science and Technology, Federal University of São Paulo, São José dos Campos 12231-280, Brazil and [6]CeRiN - Centro di Riabilitazione Neurocognitiva, Università degli Studi di Trento, Rovereto 38068, Italy

Address correspondence to Alberto Pisoni. Email: alberto.pisoni@unimib.it.

Abstract

Increasing evidence shows that anodal transcranial direct current stimulation (tDCS) enhances cognitive performance in healthy and clinical population. Such facilitation is supposed to be linked to plastic changes at relevant cortical sites. However, direct electrophysiological evidence for this causal relationship is still missing. Here, we show that cognitive enhancement occurring in healthy human subjects during anodal tDCS is affected by ongoing brain activity, increasing cortical excitability of task-related brain networks only, as directly measured by Transcranial Magnetic Stimulation combined with electroencephalography (TMS-EEG). Specifically, TMS-EEG recordings were performed before and after anodal tDCS coupled with a verbal fluency task. To control for effects of tDCS protocol and TMS target location, 3 conditions were assessed: anodal/sham tDCS with TMS over left premotor cortex, anodal tDCS with TMS over left posterior parietal cortex. Modulation of cortical excitability occurred only at left Brodmann's areas 6, 44, and 45, a key network for language production, after anodal tDCS and TMS over the premotor cortex, and was positively correlated to the degree of cognitive enhancement. Our results suggest that anodal tDCS specifically affects task-related functional networks active while delivering stimulation, and this boost of specific cortical circuits is correlated to the observed cognitive enhancement.

Key words: anodal tDCS, cortical excitability, TMS-EEG, verbal fluency

Introduction

Transcranial direct current stimulation (tDCS) is a brain stimulation technique, which is able to non-invasively increase (anodal tDCS) or decrease (cathodal tDCS) the excitability of the human cerebral cortex (Nitsche and Paulus 2000). In the last decade, several studies successfully applied tDCS to modulate a wide range of motor, perceptive, and cognitive processes, as well as to treat neurological and psychiatric diseases (Nitsche and Paulus 2011; Jacobson et al. 2012). Although human and animal works have provided several hints on the biological mechanisms driving anodal tDCS offline effects (Bindman et al. 1964; Liebetanz et al. 2002; Bikson et al. 2004; Fritsch et al. 2010), and despite its increased popularity, the neural underpinnings of tDCS effects on task performance still remain elusive. Motor-evoked potential studies showed that the neurophysiological effects induced online by anodal tDCS rely on the subthreshold depolarization of the primary motor cortex neuronal membrane, mediated by NA+ voltage-dependent ion channels activation (Liebetanz et al. 2002; Nitsche et al. 2003). Similarly, previous in vitro studies reported that this modulation of neurons

excitability increased spontaneous cortical activity (Bindman et al. 1964). Offline effects, instead, have been shown to be mediated by glutamate *N*-methyl-d-aspartate receptors activation, which results in a greater CA++ postsynaptic concentration, which triggers cortical plasticity (Nitsche and Paulus 2000, 2011). However, in humans, outside the motor domain, no evidence is reported which could directly link tDCS plastic modulation of cortical excitability to its effects on cognition. Moreover, tDCS low spatial resolution seems to be in contrast with focal effects on cognitive performance (Nitsche and Paulus 2011; Jacobson et al. 2012; Monti et al. 2012) and electrophysiological measures (Keeser et al. 2011; Wirth et al. 2011) described in many studies. Current modeling research, indeed, found that electrical currents delivered through tDCS spread well far away from the stimulation site and that micro-anatomical differences may vary its path (Datta et al. 2010; Bikson et al. 2012; Opitz et al. 2015). An activity-selectivity hypothesis for tDCS enhancement of human behavior has been repeatedly proposed but never directly tested (for a perspective review, see Bikson and Rahman 2013). The present study examines the specificity of anodal tDCS effects on brain connectivity and cortical excitability during a task execution, by means of Transcranial Magnetic Stimulation combined with electroencephalography (TMS-EEG) recordings.

As recently demonstrated, indeed, TMS-EEG recordings are able to highlight, by analyzing TMS-evoked potentials (TEPs), plastic changes in cortical excitability and connectivity during and after anodal tDCS, applied at resting state over the motor and parietal cortices (Pellicciari et al. 2013; Romero Lauro et al. 2014, 2016). However, it is unknown whether and how specific task-related spontaneous cortical activity interacts with the electrical stimulation and how this is linked with the behavioral modulations found in the literature. Animal models showed that anodal tDCS is able to modify synaptic efficiency, by inducing repetitive firing in target neurons (Bikson et al. 2004) causing an increase in extracellular ionic activity and possibly protein expression. Accordingly, further in vitro studies showed that offline effects are the result of an interaction between the spontaneous ongoing cortical activity and electrical stimulation, with the latter modulating plasticity and excitability only in those neurons which are more active during the stimulation protocol (Fritsch et al. 2010). If this is true also for humans, we should expect an increased response in terms of cortical excitability and connectivity only after testing task-related areas. Otherwise, if anodal tDCS effects are not influenced by ongoing brain activity, electrical stimulation should aspecifically increase cortical excitability of both task-related and unrelated areas. In order to test this hypothesis, we chose a verbal fluency task as our experimental tDCS-behavioral protocol since previous evidence (Cattaneo et al. 2011; Meinzer et al. 2012) suggested that anodal tDCS over the left inferior frontal gyrus (LIFG) increases performance in verbal fluency compared with a placebo condition. TMS-EEG recordings were performed measuring cortical response to magnetic perturbation of areas included (left Brodmann's area [BA] 6), or not (left BA7), in the functional network underlying verbal fluency; in this way, we aimed to assess whether the electrical stimulation protocol could induce site-specific plastic changes, or whether the neurophysiological modulation affected broader cortical regions not related to task execution.

Materials and Methods

Participants

Eighteen neurologically unimpaired individuals (8 males, mean age 27.7 years, standard deviation [SD] 5.3, range 21–38; mean years of formal education 16.2, SD 2.1, range 13–18 years) took part in the experiment. All participants were native Italian and were naive to the experimental procedure and the purpose of the study. All subjects were right-handed (mean Edinburgh handedness Inventory, Oldfield 1971 = 0.95; SD = 0.06; range = 0.79–1) and with normal or corrected-to-normal vision. Participants had no history of chronic or acute neurologic, psychiatric, or medical disease; no family history of epilepsy; no current pregnancy; no cardiac pacemaker; no previous surgery involving implants to the head (cochlear implants, aneurysm clips, brain electrodes); and did not take acute or chronic medication. Written informed consent was obtained from all participants. Each subject underwent 3 different experimental sessions designed as follows: 1) anodal tDCS over the LIFG and TMS over the left BA6; 2) sham tDCS and TMS over the left BA6; 3) anodal tDCS over the LIFG and TMS over the left PPC (for a schematic representation of experimental sessions, see Fig. 1*a*). While session 1 can be considered as the main experimental condition, sessions 2 and 3 served as controls. In particular, condition 2 controlled for specific effects of the tDCS protocol, by comparing TMS-EEG recordings performed pre and post anodal versus sham stimulation, with TMS applied over BA6. Condition 3, instead, tested the same tDCS protocol used in condition 1, but controlled for the specificity of TMS target site and for possible effects of coil proximity on neurophysiological measurements. To safely exclude this possibility, anodal tDCS was delivered over the LIFG as in session 1, but TMS targeted the left PPC, corresponding to left BA7, that is, an area not involved in the task (Weiss et al. 2003; Birn et al. 2010). Stimulation order was counterbalanced across subjects and each session was separated by a 1-week washout period. The local ethical committee of the University of Milano-Bicocca approved the experiment and subjects were treated in accordance with the Declaration of Helsinki.

Transcranial direct current stimulation

tDCS protocol was delivered by introducing the electrodes under the EEG cap. A battery-driven constant current stimulator (Eldith,

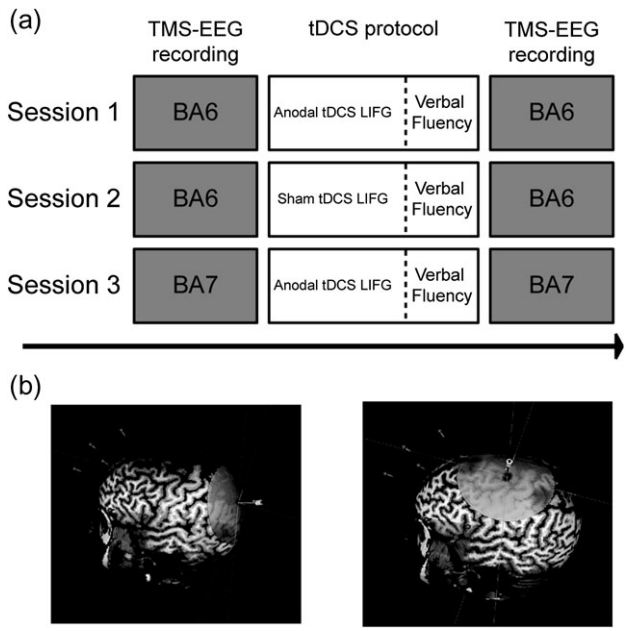

Figure 1. (*a*) Schematic representation of the experimental sessions. (*b*) NBS screenshots of the left frontal (BA6) and parietal (BA7) TMS hotspots in a representative subject.

Neuroconn) delivered the stimulation. The anode (16 cm^2) was placed over the LIFG, while the cathode (25 cm^2) was placed over the right supraorbital region. The LIFG was localized on the individual structural magnetic resonance images (MRIs) of the subject through the integrated neuro-navigation system of the TMS-EEG instrument (Eximia, Nexstim). Stimulation intensity was set at 0.75 mA resulting in a current density of 0.47 A/m^2 and charge density of 562 C/m^2 for the anode and a density of 0.3 A/m^2 and charge density of 360 C/m^2 for the cathode; the duration of stimulation was 20 min with a fade in/fade out period of 30 s. For sham stimulation, the electrodes were placed in the same positions as real tDCS, but the duration was set at 30 s. Electrodes were applied by using a conductive paste (Ten20, Weaver and Co.), which lowered electrodes impedance and helped in keeping the electrodes adherent to the scalp. After the tDCS protocol, stimulation electrodes were removed, and for the few EEG electrodes, which were displaced with this procedure (2 for the right supraorbital region and 3 for the left frontal region), impedance was controlled and adjusted to obtain optimal values (<5 kΩ). This procedure took ~3 min.

Transcranial Magnetic Stimulation combined with electroencephalography

In each session, 2 TMS-EEG recordings were performed, before and after the tDCS-task experimental protocol. TMS was delivered by means of an Eximia TMS stimulator (Nexstim) using a focal figure of eight 70-mm coil. The frontal TMS hotspot was located over the left premotor cortex (BA6, Montreal Neurological Institute [MNI] coordinates: x −16, y 4, z 68, see Fig. 1*b*). Other imaging studies reported similar coordinates for BA6 (Costafreda et al. 2006; Kircher et al. 2011; Meinzer et al. 2013). This area was chosen as TMS hotspot according to previous studies in which a greater activation of BA6 was reported for verbal fluency with respect to word repetition (Meinzer et al. 2012). The TMS hotspot (for sham and real frontal sessions) was selected in a pilot session as the site in BA6 where stimulation induced TEPs without muscular artifacts. The parietal TMS target was set over the left superior parietal lobule (BA7, see Fig. 1*b*), an area not involved in the functional network specific for verbal fluency (Weiss et al. 2003; Birn et al. 2010). High-resolution (1 × 1 × 1 mm) structural MRIs were acquired for each participant using a 3-T Intera Philips body scanner (Philips Medical Systems). The TMS target was identified on individual MRIs using an integrated Navigated Brain Stimulation (NBS) system (Nexstim), which employs infrared-based frameless stereotaxy, in order to map the position of the coil and of the participant's head, within the reference space of the individual's MRI space. The NBS system allowed to continuously monitor the position and orientation of the coil, thus assuring precision and reproducibility of the stimulation across recordings. Moreover, the NBS system estimated online the intensity (V/m) of the intracranial electric field induced by TMS at the stimulation hotspot, accounting for the head and brain shape of each participant, and taking into consideration the distance from scalp and coil position. In each session, TMS intensity was delivered at an intensity eliciting an estimated electrical field at the hotspot of 95 V/m. This resulted in a mean intensity of 62% of the maximum stimulator output (SD 5.7; range 50–70%). Critically, TMS intensity was kept constant for pre- and post-tDCS recording for each subject within each session. Wilcoxon nonparametric tests showed no difference in TMS intensity between sessions (all $Ps > 0.11$). TMS single pulses were delivered at an interstimulus interval randomly jittering between 2100 and 2300 ms. In all, 180 trials were acquired for each recording.

EEG Recording During TMS

EEG signal was continuously recorded using a TMS compatible 60-channels amplifier (Nexstim Ltd.), which prevents saturation by means of a proprietary sample-and-hold circuit that holds the amplifier output constant from 100 μs pre- to 2 ms post-TMS pulse (Virtanen et al. 1999). Two electrodes placed over the forehead were used as ground. Eye movements were recorded by means of 2 additional electrodes placed near the eyes in order to monitor ocular artifacts. As in previous studies, during EEG recordings, participants wore earplugs and heard a continuous masking noise to cover TMS coil discharge (Massimini et al. 2005; Casarotto et al. 2010; Romero Lauro et al. 2014), avoiding thus the emergence of auditory-evoked potentials. Electrodes impedance was kept below 5 kΩ, and EEG signals were recorded with a sampling rate of 1450 Hz.

Data preprocessing was carried out using Matlab R2012a (Mathworks). Data were down-sampled to 725 Hz, continuous signal was split in epochs starting 800 ms pre- and ending 800 ms post-TMS pulse. Trials with excessive artifacts were removed by visual inspection (Casali et al. 2010) and a band-pass filter between 2 and 80 Hz was applied as well as a notch filter at 50 Hz. TEPs were computed by averaging selected artifact-free single epochs. Bad channels were interpolated using spherical interpolation function of EEGLAB (Delorme & Makeig 2004). TEPs were then referenced and baseline corrected between −300 and −50 ms before the TMS pulse.

For each recording, as a measure of cortical excitability, global mean field power (GMFP) was computed on the averaged TEP signal recorded from all 60 EEG channels (as in Romero Lauro et al. 2014). GMFP is considered a reliable measure of cortical excitability and connectivity of the targeted area and of the related functional network (Massimini et al. 2005; Rosanova et al. 2009; Casarotto et al. 2010; Mattavelli et al. 2013; Romero Lauro et al. 2014). Similarly, local mean field power (LMFP) was computed to specifically assess cortical excitability of a restricted scalp area (Pellicciari et al. 2013; Romero Lauro et al. 2014). In particular, LMFP was computed for 6 different electrode clusters, defined on the basis of their anatomical position. The first one included the 2 electrodes directly interested by the tDCS anode, over the LIFG (C1, electrodes F5–F7). Cluster 2 included the electrodes above the frontal TMS hotspot (BA6), therefore under the TMS coil (C2, electrodes F1–FC1). Cluster 3 included the electrodes over the parietal TMS hotspot (C3, CP1-P1). Clusters 4, 5, and 6 represented the contralateral sites of C1, C2, and C3, respectively (see Supplementary Fig. 2). GMFP and LMFP were computed for the whole considered TEP duration (0–150 ms) and for 3 time windows, identified in order to separately analyze early and late TEP components: 0–30 ms; 30–65 ms, and 65–150 ms.

To better refine the spatial resolution of the highlighted findings and to account for possible effects of volume conduction in the EEG signal, source modeling was performed following the procedures in Casali et al. (2010) and Romero Lauro et al. (2016). First, meshes of cortex, skull, and scalp compartments (containing 3004, 2000, and 2000 vertices, respectively) were obtained starting from individual MRIs to represent conductive head volume, and were modeled following the 3-spheres BERG method (Berg and Scherg 1994), which is implemented in the Brainstorm software package (http://neuroimage.usc.edu/brainstorm, last accessed January 27, 2017). This method includes 3 concentric spheres

with different homogeneous conductivities, each representative of the best-fitting sphere of inner skull, outer skull, and scalp compartments. Then, the model was constrained to the cortex, reconstructed as a 3D grid of 3004 fixed normally oriented dipoles with respect to the cortical surface. Finally, EEG sensor positions recorded during the TMS-EEG sessions were coregistered with the meshes, using rotations and translations of digitized landmarks identified on the individual MRI (nasion, left and right tragus). Then, the inverse transformation was applied to the MNI canonical mesh of the cortex for approximating the real anatomy. For each participant, the inverse solution was computed on each artifact-free TMS/EEG trial using the weighted minimum norm estimate with Gaussian geodesic smoothness prior (Casali et al. 2010). After source reconstruction, a statistical threshold was computed in order to assess when and where the post-TMS cortical response differed from pre-TMS activity (i.e., to identify TMS-evoked response). To do so, a nonparametric permutation-based procedure was applied (Pantazis et al. 2003). A binary spatial-temporal distribution of statistically significant sources was obtained and thus only information from significant cortical sources was used for further analyses. As indices of cortical activity, we cumulated the absolute significant current density (global SCD, measured in $\mu A/mm^2$, Casali et al. 2010) over all 3004 cortical vertexes and over the 3 time windows of interest (0–30 ms, 30–65 ms and 65–150 ms) for each recording session (6: pre and post each experimental session). Finally, in order to mirror the LMFP analysis of the sensor data, for each experimental condition, we computed a local SCD in the vertexes within 6 different BAs, identified by means of an automatic tool of anatomical classification (WFUPickAtlas tool; http://www.ansir.wfubmc.edu, last accessed January 27, 2017; Maldjian et al. 2003, 2004). These BAs approximately corresponded to the 6 LMFP clusters identified in sensor analysis (left/right BAs 44/45, 6, and 7, as in Casali et al. 2010; Romero Lauro et al. 2016).

Verbal Fluency

In each session, participants performed the fluency task with 2 semantic and 2 phonemic cues. In particular, they were asked to produce in 1 min as many words as they could beginning with a given letter or belonging to a specific semantic category. Subjects were also asked not to produce the same word twice and to stick as much as possible to the noun grammatical category. Letters were presented in fixed pairs ("P" and "G," "D" and "L," "F" and "C") balanced according to the relative frequency of names beginning with each pair of letters, as derived from the Corpus and Frequency Lexicon of Written Italian (COLFIS, see http://www.istc.cnr.it/material/database/colfis/index_eng.shtml, last accessed January 27, 2017). Category pairs were "Clothing" and "Vegetables," "Animals" and "Tools," and "Vehicles" and "Fruits." As for letters, they were matched according to a pilot study performed on 10 healthy subjects in order to have 1) a similar number of words produced per each category pair and 2) a living and a nonliving category in each session. Letters and categories pairs order was counterbalanced across sessions and stimulation condition, in order to have subjects performing the fluency task with different letters and categories in each experimental session.

Analyses

Analyses were run with the statistical programming environment R (R Core Team, 2014). Linear mixed-effect models were adopted as the main statistical procedure (Baayen et al. 2008). As our data involved a continuous dependent variable, namely number of produced words, TEP values and SCD values, a series of linear mixed-effects regression using LMER procedure in "lme4" R package (version 1.1-5, Bates et al. 2014) were performed. Fixed effects inclusion in the final model has been tested with a series of likelihood ratio tests, including each effect which significantly increased the model's goodness of fit (Gelman and Hill 2006). Concerning the behavioral performance, the considered fixed effects were stimulation session (factorial, 3 levels: Real tDCS-frontal TMS, Real tDCS-parietal TMS, and sham tDCS) and fluency type (factorial, 2 levels: semantic and phonemic fluency) and their interaction. Concerning the random effect structure, a by-subjects random intercept was included. GMFP, LMFP, and SCD values were submitted to a similar procedure. Concerning GMFP, models were estimated by including stimulation session (factorial, 3 levels: anodal tDCS-TMS BA6, anodal tDCS-TMS BA7, and sham tDCS) and recording time (factorial, 2 levels: pre- and post-tDCS) as fixed effects on each time window. Concerning the random effect structure, a by-subjects intercept was included. The same procedure was adopted for global SCD. Concerning LMFP and local SCD, the same procedure was adopted, and data were separately analyzed for clusters. Once the final model was defined, an ANOVA was run on it, which will be reported with significance levels based on Satterthwaite's degrees of freedom approximation in "lmerTest" R package (version 2.0-6, Kuznetsova et al. 2015). Lastly, to directly contrast single levels of the significant interactions and main effects, post hoc procedures were carried out on the best-fitting final model with the "phia" R package (version 0.2-0, De Rosario-Martinez 2015), applying Bonferroni–Holm correction for multiple comparisons. To assess whether the increase in indices of cortical excitability was associated with the behavioral performance in the verbal fluency task, one-tailed correlations were run between increase in neurophysiological responses and behavioral performance. For the neurophysiological increment index, we subtracted the increment in local SCD between pre and post sham tDCS recordings (SCD post-tDCS − SCD pre-tDCS) to the increment in local SCD between pre and post real tDCS recordings, separately for both BA6 and BA7 sessions. We then computed the index of behavioral enhancement by subtracting the verbal fluency score in the sham session to the verbal fluency score in the real sessions, separately for BA6 and BA7 sessions. Correlations between the behavioral and neurophysiologic enhancement (in each considered BA) were run and 90% confidence intervals were obtained for significant correlations by a 1000 permutation bootstrap procedure in R with the "boot" function.

Results

Verbal Fluency

At a behavioral level, scores were higher for semantic fluency (17.9 words, SD = 3.3) as compared with phonemic one (15.8 words, SD = 3.5; $F_{1,85} = 10.5$; $P = 0.002$). Interestingly, as expected, anodal tDCS significantly enhanced verbal fluency. The main effect of stimulation, indeed, was significant ($F_{2,85} = 7.4$; $P = 0.001$). In particular, placebo stimulation sessions resulted in lower fluency scores (15.2 words, SD = 2.7) compared with both sessions in which anodal tDCS over the LIFG was delivered (TMS BA6: 17.9 words, SD = 4.2; $P < 0.001$; TMS BA7: 17.5 words, SD = 3.3; $P = 0.003$; See Fig. 2). As previously reported (Cattaneo et al. 2011), the stimulation by type of fluency interaction was not significant ($F_{2,85} = 0.18$; $P = 0.84$).

GMFP and LMFP

Concerning global cortical excitability, measured as GMFP, the stimulation by recording time interaction resulted significant ($F_{2,85}$ = 3.59; P = 0.03). Post hoc analyses showed that cortical excitability significantly increased in post anodal tDCS compared with pre-tDCS recordings when TMS was applied over BA6 (P = 0.013), while no change was detected in sham sessions (P = 0.99) and in anodal tDCS sessions, when TMS was applied over BA7 (P = 0.93). These results strongly corroborate the hypothesis that anodal tDCS acts by increasing cortical excitability of the cerebral cortex even outside the primary motor cortex (Fig. 3*a*).

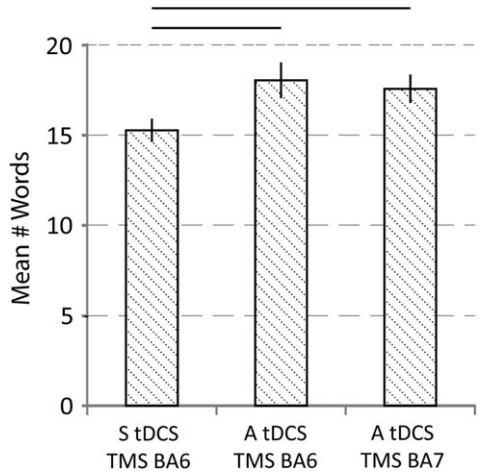

Figure 2. Behavioral results of the verbal fluency tasks: mean produced words in the 3 experimental sessions. Performance improved after anodal tDCS. Error bars represent ± 1 SEM.

In order to better assess how cortical excitability was modulated by the application of tDCS, we analyzed the modulation of TEPs within 3 time windows based on the grand average of the GMFP: 0–30 ms (early latency), 30–65 ms (middle latency), and 65–150 ms (late latency). The stimulation by recording time interaction was significant in the early–latency TEP component ($F_{2,51}$ = 3.78; P = 0.03), where an increase in global cortical excitability was detectable in post-tDCS as compared with pre-tDCS recordings in real tDCS-BA6 sessions (P < 0.001, see Fig. 3*a*). This early component reflects cortical excitability of the targeted area (Ilmoniemi and Kicic 2010; Pellicciari et al. 2013). Similarly, TEP increased in the middle-latency component ($F_{2,68}$ = 3.8; P = 0.026), only after anodal tDCS TMS over BA6 sessions (P = 0.01) while no difference was highlighted in the other sessions (sham: P = 0.95; BA7: P = 0.84).

In order to roughly localize the cortical excitability increase, we computed, for each time window, the LMFP for different electrodes clusters, namely C1 near the anode, C2 near the TMS coil, and C3 over an area which was not involved in the task but near coil location in the control session (i.e., PPC). Homologous clusters on the contralateral hemisphere were also investigated (C4, C5, and C6; see Supplementary Fig. 1). For the early-latency component, analyses showed a significant increase in LMFP in C1, that is, near the anode location only after real tDCS sessions with TMS applied over BA6 (P < 0.001), confirming tDCS-specific effect on the stimulated area, while no effect was highlighted in sham sessions (P = 1) or when TMS was applied over BA7 (P = 0.1). Similarly, C2 showed the same increase in LMFP in the early-latency component (anodal tDCS-BA6: P = 0.007; anodal tDSC-BA7: P = 1; Sham: P = 1). Concerning the middle-latency component, which reflects functional network cortical excitability properties (Casarotto et al. 2010; Ilmoniemi and Kicic 2010; Veniero et al. 2012), a greater post-tDCS TEP was found for C2, near the TMS coil (i.e., left

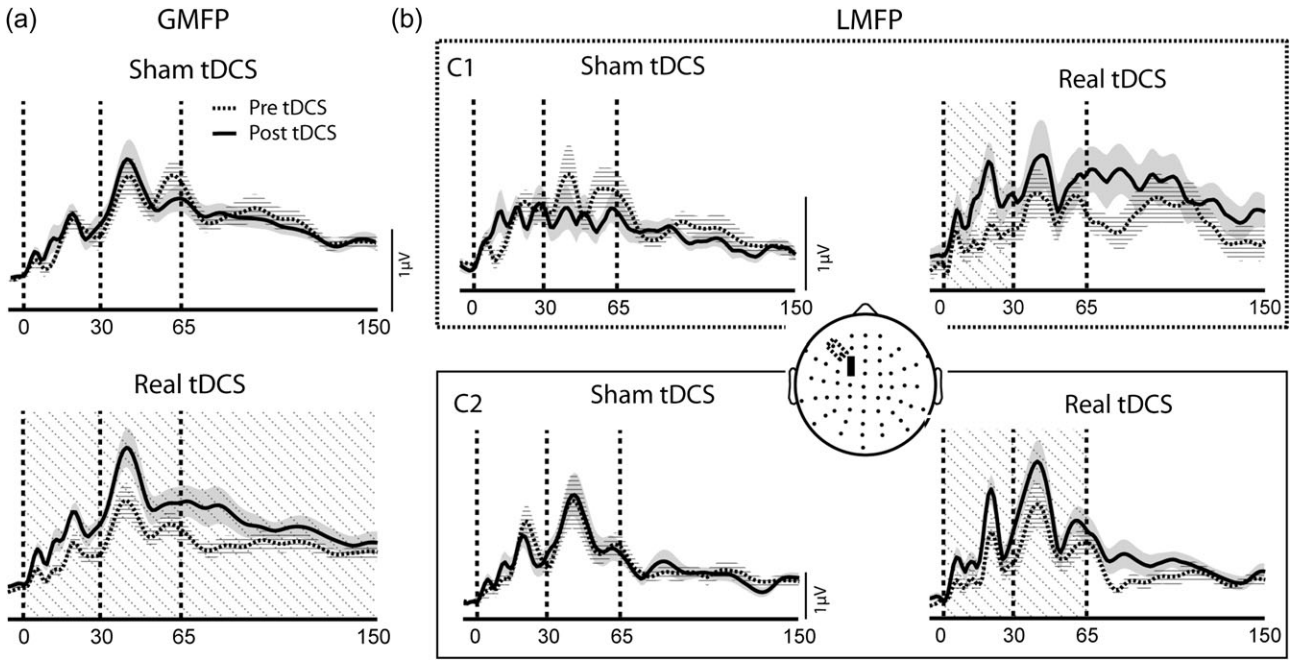

Figure 3. Grand average results from the GMFP and LMFP analyses. Traces represent mean GMFP/LMFP ± 1 SEM. Dot-shaded areas indicate significant differences. (*a*) GMFP in pre- and post-tDCS recordings in Sham (upper row) and anodal tDCS/TMS over left BA6 (lower row) sessions. Global cortical excitability increased after real stimulation in the early and middle TEP component. (*b*) LMFP of Cluster 1 (dotted box) and Cluster 2 (solid box), as highlighted in the central head model. In C1, LMFP increased after anodal tDCS/TMS over BA6 in the early component. In C2, LMFP increased after anodal tDCS/TMS over BA6 in the early- and middle-latency component.

BA6, $P < 0.001$) only in anodal tDCS sessions with TMS applied over BA6. In sham sessions, and when TMS was applied over BA7 no increase was reported between pre- and post-tDCS recordings (both Ps = 1). For the late-latency components, no increase was highlighted in any considered cluster (Fig. 3*b*).

SCD and Local SCD

Confirming the spatial specificity of the effects of stimulation (see Fig. 4*c–f*), left BA6 and BA44/45 were the only cortical sites in which an increase in cortical excitability was detectable. In particular, for left BA6, the stimulation by recording session interaction was significant ($F_{2,51} = 3.9$; $P = 0.027$), since post-tDCS recordings in anodal stimulation sessions with TMS over BA6 resulted in an increase in SCD when compared with pre-tDCS recordings ($P = 0.014$), while no difference was present for sham ($P = 0.96$) and anodal sessions with TMS over BA7 ($P = 0.97$). The same result was found for left BA44/45 ($F_{2,51} = 3.1$; $P = 0.05$); post hoc analysis showed a significant difference between pre and post real tDCS sessions with TMS applied over BA6 ($P = 0.01$), while no difference was present between pre and post sham ($P = 0.97$) and BA7 ($P = 0.98$) sessions (see Fig. 4*c*,*e*).

Finally, to further investigate the link between cognitive and neurophysiological tDCS-driven enhancement, we computed the correlation between the enhancement in verbal fluency performance and cortical excitability increase between pre- and post-tDCS protocols. Our results indicate a positive correlation between the increase in SCD in left BA44/45 after anodal tDCS and TMS applied over left BA6 and the increase in verbal fluency performance in that session ($r = 0.53$; $P = 0.012$, Bootstrap 90% CI = 0.38 0.79; see Fig. 5). To our knowledge, this is the first time that a direct measure of brain excitability is linked to a modulation of a cognitive performance, and the first, in vivo, evidence that neurophysiological and cognitive effects of tDCS are correlated (for correlations with indirect metabolic measures, see Holland et al. 2011; Meinzer et al 2012).

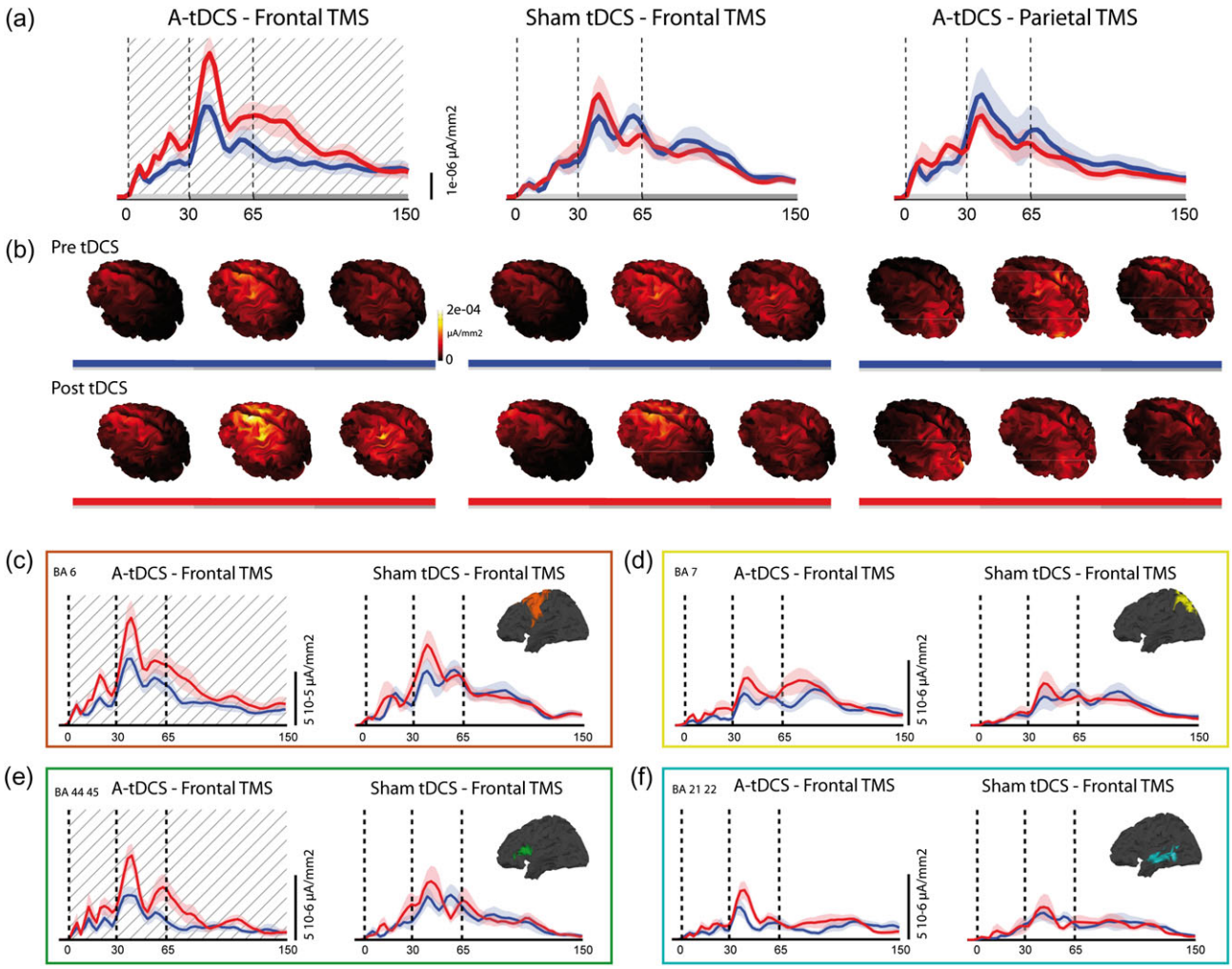

Figure 4. Grand average results from the global and local source modeling. Traces represent mean SCD/Local SCD ± 1 SEM. Dot-shaded areas indicate significant differences. (*a*) Plots of the SCD over time in pre- (blue line) and post- (red line) tDCS recordings. Significant difference in pre–post-tDCS cortical activity is evident only for anodal tDCS sessions with TMS applied over left BA6 (first plot), while no difference is highlighted for sham tDCS sessions (second plot) or when TMS was applied over the left BA7. (*b*) Source localization of the global cortical activity. The increment in local SCD is evident in left premotor areas after anodal tDCS with TMS over left BA6. (*c–f*) SCD in left BA6 (*c*, orange box), left BA44,45 (*e*, green box), left BA7 (*d*, yellow box), and left BA21/22 (*f*, cyan box) in pre (blue line) and post (red line) sham and anodal tDCS sessions, while probing cortical excitability from left BA6. Differences between pre- and post-tDCS sessions are highlighted only for anodal tDCS sessions in left BA6 and 44/45.

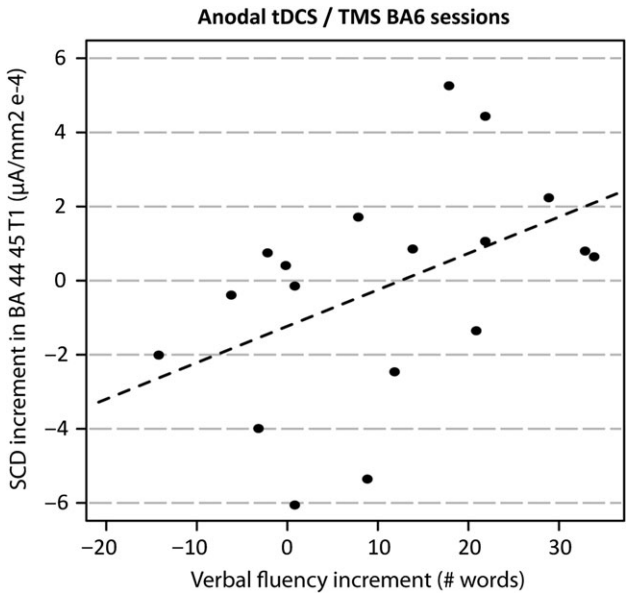

Figure 5. Scatterplot illustrating the significant correlation between the increase in verbal fluency performance, compared with sham sessions, and the increase in SCD in left BAs 44/45 during the anodal tDCS session with cortical excitability probed from left BA6.

Discussion

The present results define how, at a functional level, tDCS affects cortical circuits when the stimulation is applied during task performance. At a behavioral level, anodal tDCS increased verbal fluency performance. Concurrently, both global and local neurophysiological measurements showed a significant increase only when triggered from left BA6, which is part of the verbal fluency functional network. This increment was highlighted in the early TEP component, which is considered a direct and reliable marker of cortical excitability of the targeted area (Ilmoniemi and Kicic 2010; Pellicciari et al. 2013), for the electrode clusters over the LIFG and over the left BA6, and in the middle-latency component, an index of excitability of the functional network activated by the task (Casarotto et al. 2010; Ilmoniemi and Kicic 2010; Veniero et al. 2012) for the electrodes cluster over the left BA6. Source analysis confirmed the specificity of the effects of stimulation (see Fig. 4*c–f*), since left BA6 and BA44/45 were the only cortical sites in which an increase in cortical excitability was detectable between pre and post anodal tDCS recordings when TMS was applied over BA6. As Figure 4*b* shows, the topography of this tDCS-induced cortical enhancement when TMS was applied over BA6 is restricted to functionally related sites, and the peak of activation is not directly under the tDCS patch but, as suggested by current modeling studies (Datta et al. 2010; Bikson et al. 2012; Opitz et al. 2015), rather between the anode and the cathode. No increase of cortical excitability, instead, was detected when TMS was delivered over BA7, a region not involved in the task, thus ruling out the possibility that tDCS local effects were due to magnetic stimulation proximity. Similarly, no change was detected when sham tDCS was delivered, confirming that the increase in cortical excitability recorded in real tDCS sessions was due to an interaction between neurophysiological modulation and cortical activity elicited by cognitive processing. Overall, the present results showed that, while performing a language production task, anodal tDCS induces cortical plastic changes only in those areas which are relevant for task execution. The implication of the present findings is striking, since they suggest that even if electrical currents delivered by tDCS spread far away from the stimulation site, as suggested by modeling studies (Datta et al. 2010; Bikson et al. 2012; Opitz et al. 2015), their functional effects are restricted to those areas which are more active during the stimulation protocol. This evidence seems at odds with a previous TMS-EEG study showing that at rest, after right parietal tDCS, cortical excitability increased in bilateral frontal and parietal sites (Romero Lauro et al. 2014). However, this fronto-parietal cortical pattern overlaps the default mode network, which is assumed to be active when no specific task is performed.

One plausible reason determining the site specificity of functional effects can be found in tDCS online and offline mechanisms of action: neurophysiological modulation induced by the stimulation is strictly connected to spontaneous firing and synaptic efficacy (Bindman et al. 1964; Nitsche and Paulus 2000; Bikson et al. 2004; Fritsch et al. 2010). If the area is not activated by task execution concurrently with tDCS applications, thus, no plastic change is detectable. Animal model supports this view by showing that M1 mouse slices needed simultaneous DC and synaptic activation in order to induce Long Term Potentiation-like changes (Fritsch et al. 2010). According to this view, the areas involved in the execution of our verbal fluency task (left BA6, BA44, and BA45), which more likely exhibited an increase in synaptic activity during the stimulation protocol, showed an offline increment in cortical excitability, while areas outside the functional network of verbal fluency (left BA7) did not show any neurophysiological modulation. These findings, by supporting the activity-selectivity hypothesis (Bikson and Rahman 2013), confirm in humans what was found in animal models, representing a solid theoretical framework for designing future experiments involving anodal tDCS and for interpreting past and future results obtained with this non-invasive brain stimulation technique. It has to be noted, however, that more than electrodes location, what may be crucial for the observed neurophysiological modulation could be current flow direction, which may alter the neural input/output (I/O) function (Lafon et al. 2016). Technically speaking, thus, defining the present protocol as "anodal" may be misleading, since any tDCS protocol with cephalic reference includes an anode and a cathode. However, while computational models provided evidence for an increased I/O function for the areas under the anode, they do not show significant effects on areas under the cathode, at least for the classical motor cortex montage (Lafon et al. 2016).

Another relevant result of the present work is that the modulation of the performance at the verbal fluency task and the cortical excitability increase occurring in left BAs 44 and 45 significantly correlated. To our knowledge, this is the first time that a direct measure of brain excitability is linked to the modulation of a cognitive performance, and the first, in vivo, evidence that neurophysiological and cognitive effects of tDCS are correlated. Our data suggest, thus, a strict link between the tDCS-induced enhancement in performance on the verbal fluency task and plastic changes occurring at specific cortical sites.

Taken together, by shedding light on the site specificity of tDCS neurophysiological effects on cortical plasticity and their relationship with cognitive functions enhancement, the present results offer a theoretical framework in which non-invasive brain stimulation literature could interpret its findings and may help in designing more effective tDCS protocols aimed at treating neurological and psychiatric conditions and study

diseases hallmarked by abnormal cognitive functioning and neurophysiological responses.

Supplementary Material

Supplementary material is available at *Cerebral Cortex* online.

Notes

Conflict of Interest: None declared.

References

Baayen RH, Davidson DJ, Bates DM. 2008. Mixed-effects modeling with crossed random effects for subjects and items. J Mem Lang. 59:390–412.

Bates D, Maechler M, Bolker B, Walker S. lme4: linear mixed-effects models using Eigen and S4. R package version 1.1-7. 2014. Available from: URL http://CRAN.R-project.org/package=lme4 (last accessed January 27, 2017).

Berg P, Scherg M. 1994. A fast method for forward computation of multiple-shell spherical head models. Electroencephalogr Clin Neurophysiol. 90:58–64.

Bikson M, Inoue M, Akiyama H, Deans JK, Fox JE, Miyakawa H, Jefferys JG. 2004. Effects of uniform extracellular DC electric fields on excitability in rat hippocampal slices in vitro. J Physiol. 557:175–190.

Bikson M, Rahman A, Datta A. 2012. Computational models of transcranial direct current stimulation. Clin EEG Neurosci. 4:176–183.

Bikson M, Rahman A. 2013. Origins of specificity during tDCS: anatomical, activity-selective, and input-bias mechanisms. Front Hum Neurosci. 7:688.

Bindman LJ, Lippold OCJ, Redfearn JWT. 1964. The action of brief polarizing currents on the cerebral cortex of the rat during current flow and in the production of long-lasting after-effects. J Physiol. 172:360–382.

Birn RM, Kenworthy L, Case L, Caravella R, Jones TB, Bandettini PA, Martin A. 2010. Neural systems supporting lexical search guided by letter and semantic category cues: a self-paced overt response fMRI study of verbal fluency. NeuroImage. 49:1099–1107.

Casali AG, Casarotto S, Rosanova M, Mariotti M, Massimini M. 2010. General indices to characterize the electrical response of the cerebral cortex to TMS. NeuroImage. 49:1459–1468.

Casarotto S, Romero Lauro LJ, Bellina V, Casali AG, Rosanova M, Pigorini A, Defendi S, Mariotti M, Massimini M. 2010. EEG responses to TMS are sensitive to changes in the perturbation parameters and repeatable over time. PLoS One. 5:e10281.

Cattaneo Z, Pisoni A, Papagno C. 2011. Transcranial direct current stimulation over Broca's region improves phonemic and semantic fluency in healthy individuals. Neuroscience. 183:64–70.

Costafreda SG, Fu CHY, Lee L, Everitt B, Brammer MJ, David AS. 2006. A systematic review and quantitative appraisal of fMRI studies of verbal fluency: role of the left inferior frontal gyrus. Hum Brain Mapp. 27:799–810.

Datta A, Bikson M, Fregni F. 2010. Transcranial direct current stimulation in patients with skull defects and skull plates: high-resolution computational FEM study of factors altering cortical current flow. Neuroimage. 52:1268–1278.

Delorme A, Makeig S. 2004. EEGLAB: an open source toolbox for analysis of single-trial EEG dynamics including independent component analysis. J Neurosci Methods. 134:9–21.

De Rosario-Martinez H phia: Post-Hoc Interaction Analysis. R package version 0.2-0. 2015. Available from: URL http://CRAN.R-project.org/package=phia (last accessed January 27, 2017).

Fritsch B, Reis J, Martinowich K, Schambr HM, Ji Y, Cohen LG, Lu B. 2010. Direct current stimulation promotes BDNF-dependent synaptic plasticity: potential implications for motor learning. Neuron. 66:198–204.

Gelman A, Hill J. 2006. Data analysis using regression and multilevel/hierarchical models. New York: Cambridge University Press.

Holland R, Leff AP, Josephs O, Galea JM, Desikan M, Price CJ, Rothwell JC, Crinion J. 2011. Speech facilitation by left inferior frontal cortex stimulation. Curr Biol. 21:1403–1407.

Ilmoniemi RJ, Kicic D. 2010. Methodology for combined TMS and EEG. Brain Topogr. 22:233–248.

Jacobson L, Koslowsky M, Lavidor M. 2012. tDCS polarity effects in motor and cognitive domains: a meta-analytical review. Exp Brain Res. 216:1–10.

Keeser D, Padberg F, Reisinger E, Pogarell O, Kirsch V, Palm U, Karch S, Moller HJ, Nitsche MA, Mulert C. 2011. Prefrontal direct current stimulation modulates resting EEG and event-related potentials in healthy subjects: a standardized low resolution tomography (sLORETA) study. NeuroImage. 55:644–657.

Kircher T, Nagels A, Kirner-Veselinovic A, Krach S. 2011. Neural correlates of rhyming vs. lexical and semantic fluency. Brain Res. 1391:71–80.

Kuznetsova A, Brockhoff PB, Christensen RHB lmerTest: tests in linear mixed effects models. R package version 2.0-29. 2015. Available from: URL http://CRAN.R-project.org/package=lmerTest (last accessed January 27, 2017).

Lafon B, Rahman A, Bikson M, Parra LC. 2016. Direct Current Stimulation alters neuronal input/output function. Brain Stimul. 10:36–45.

Liebetanz D, Nitsche MA, Tergau F, Paulus W. 2002. Pharmacological approach to the mechanisms of transcranial DC-stimulation-induced after-effects of human motor cortex excitability. Brain. 125:2238–2247.

Maldjian JA, Laurienti PJ, Kraft RA, Burdette JH. 2003. An automated method for neuroanatomic and cytoarchitectonic atlas-based interrogation of fMRI data sets. Neuroimage. 19:1233–1239.

Maldjian JA, Laurienti PJ, Burdette JH. 2004. Precentral gyrus discrepancy in electronic versions of the Talairach atlas. Neuroimage. 21:450–455.

Massimini M, Ferrarelli F, Huber R, Esser SK, Singh H, Tononi G. 2005. Breakdown of cortical effective connectivity during sleep. Science. 309:2228–2232.

Mattavelli G, Rosanova M, Casali AG, Papagno C, Romero Lauro LJ. 2013. Top-down interference and cortical responsiveness in face processing: a TMS-EEG study. NeuroImage. 76:24–32.

Meinzer M, Antonenko D, Lindenberg R, Hetzer S, Ulm L, Avirame K, Flaisch T, Floel A. 2012. Electrical brain stimulation improves performance by modulating functional connectivity and task specific activation. J Neurosci. 32:1859–1866.

Meinzer M, Lindenberg R, Antonenko D, Flaisch T, Flöel A. 2013. Anodal transcranial direct current stimulation temporarily

reverses age-associated cognitive decline and functional brain activity changes. J Neurosci. 33:12470–12478.

Monti A, Ferrucci R, Fumagalli M, Mameli F, Cogiamanian F, Ardolino G, Priori A. 2012. Transcranial direct current stimulation (tDCS) and language. J Neurol Neurosurg. 84: 832–842.

Nitsche MA, Paulus W. 2000. Excitability changes induced in the human motor cortex by weak transcranial direct current stimulation. J Physiol. 527:633–639.

Nitsche MA, Paulus W. 2011. Transcranial direct current stimulation – update 2011. Restor Neurol Neurosci. 29:463–492.

Nitsche MA, Fricke K, Henschke U, Schlitterlau A, Liebetanz D, Lang N, Henning S, Tergau F, Paulus W. 2003. Pharmacological modulation of cortical excitability shifts induced by transcranial direct current stimulation in humans. J Physiol. 553:293–301.

Oldfield RC. 1971. The assessment and analysis of handedness: the Edinburgh inventory. Neuropsychologia. 9:97–113.

Opitz A, Paulus W, Will S, Antunes A, Thielscher A. 2015. Determinants of the electric field during transcranial direct current stimulation. Neuroimage. 109:140–150.

Pantazis D, Nichols TE, Baillet S, Leahy RM 2003. Spatiotemporal localization of significant activation in MEG using permutation tests. In: Biennial International Conference on Information Processing in Medical Imaging. Berlin Heidelberg: Springer. p. 512–523.

Pellicciari MC, Brignani D, Miniussi C. 2013. Excitability modulation of the motor system induced by transcranial direct current stimulation: a multimodal approach. Neuroimage. 83: 569–580.

R Core Team. 2014. R: a language and environment for statistical computing. Vienna, Austria: R Foundation for Statistical Computing. Available from: URL http://www.R-project.org/ (last accessed January 27, 2017).

Romero Lauro LJ, Pisoni A, Rosanova M, Casarotto S, Mattavelli G, Bolognini N, Vallar G. 2016. Localizing the effects of anodal tDCS at the level of cortical sources: a reply to Bailey et al. Cortex. 74:323–328.

Romero Lauro LJ, Rosanova M, Mattavelli G, Convento S, Pisoni A, Opitz A, Bolognini N, Vallar G. 2014. TDCS increases cortical excitability: direct evidence from TMS–EEG. Cortex. 58:99–111.

Rosanova M, Casali AG, Bellina V, Resta F, Mariotti M, Massimini M. 2009. Natural frequencies of human corticothalamic circuits. J Neurosci. 29:7679–7685.

Veniero D, Bortoletto M, Miniussi C. 2012. Cortical modulation of short-latency TMS-evoked potentials. Front Hum Neurosci. 6:352.

Virtanen J, Ruohonen J, Näätänen R, Ilmoniemi RJ. 1999. Instrumentation for the measurement of electric brain responses to transcranial magnetic stimulation. Med Biol Eng Comput. 37:322–326.

Weiss EM, Siedentopf C, Hofer A, Deisenhammer EA, Hoptman MJ, Kremser C, Golaszewski S, Felber S, Fleischhacker WW, Delazer M. 2003. Brain activation pattern during a verbal fluency test in healthy male and female volunteers: a functional magnetic resonance imaging study. Neurosci Lett. 352:191–194.

Wirth M, Abdel Rahman R, Kuenecke J, Koenig T, Horn H, Sommer W, Dierks T. 2011. Effects of transcranial direct current stimulation (tDCS) on behaviour and electrophysiology of language production. Neuropsychologia. 49: 3989–3998.